25. GEOCHEMISTRY OF INTERSTITIAL WATERS[1]

Joris M. Gieskes,[2] Dan Schrag,[3] Lui-Heung Chan,[4] Libo Zhang,[4] and Rick W. Murray[5]

ABSTRACT

This study investigates the distribution of the inorganic constituents in the interstitial waters obtained in drill sites of the Ocean Drilling Program (ODP) Leg 152 in the Irminger Sea and off the east coast of Greenland. These studies are accompanied by detailed analyses of the distribution of the oxygen isotopes of the interstitial waters as well as by the strontium isotope $^{87}Sr/^{86}Sr$ ratio of the dissolved strontium in Sites 918 and 919. In the shelf Sites 914–916 and in the basin Site 918 there is evidence for the input of meteoric waters in the deeper parts of the drill holes, probably originating from reservoirs in the underlying basement rocks, which were subaerially deposited in Paleocene time. Strontium isotopic studies indicate several depth horizons where reaction between pore waters and volcanic material alter contemporaneous seawater signatures. All sites show evidence for a substantial input of volcanic material, typically showing considerably enhanced ratios of titanium over aluminum in the sediment. Lithium isotopes, for the first time determined in detail in ODP sites, indicate a complex pattern, suggesting reactions and exchange with the solid phases. The complex pattern will be of interest to future studies of the distribution of this isotopic ratio. Oxygen isotopic studies, in addition to showing evidence for meteoric water inputs at depth, show two other important features: (1) In the upper sediment column higher than present $\delta^{18}O(H_2O)$ values indicate the presence of a predicted glacial maximum in the isotopic composition in seawater; a chloride maximum also typically occurs, but at a depth somewhat different from that of $\delta^{18}O(H_2O)$, mostly because of different diffusive boundary conditions. (2) A minimum in $\delta^{18}O(H_2O)$ occurs at about 250 meters below seafloor (mbsf) in Site 918, a phenomenon not expected from the distribution of the inorganic constituents. Instead of a minimum at about 550 mbsf, where concentration extrema in calcium, magnesium, and chloride imply the involvement of alteration of volcanic ash, no distinct extremum in $\delta^{18}O(H_2O)$ is detected.

INTRODUCTION

During Leg 152 interstitial waters were obtained from a series of drill sites along a transect from shallow water depth across the Greenland shelf (Sites 914–916) into the Irminger Basin (Sites 918 and 919; Fig. 1). The particular aim of the program was to detect processes that affect the interstitial water chemistry and that may occur in the sediments or in the underlying basement rocks. Preliminary data have been reported in the Leg 152 *Initial Reports*. In this paper, we provide a review of the salient features of those earlier observations (Larsen, Saunders, Clift, et al., 1994) in addition to data based on the analyses of the oxygen isotopic composition of the interstitial waters (D. Schrag) and the isotopic composition of dissolved strontium and lithium (L-H. Chan and L. Zhang).

Whereas sampling for interstitial waters was sporadic at Sites 914–915, mainly as a result of low sediment recoveries, the density of the data distribution at Sites 918 and 919 allows a more detailed evaluation of the processes that affect the distribution of the dissolved constituents of the interstitial waters. We summarize the data on the shelf sites separate from the data on the Irminger Basin sites, although some similarities in processes affecting the interstitial waters may have occurred.

Unfortunately, penetration at Site 914 was poor, and drilling was discontinued well above the basement. On the other hand, both Sites 915 and 916 terminated in originally subaerial basaltic basement. Basement was reached at Site 918, but only the upper 140 m of the sediment column was cored at Site 919. This allowed a detailed sampling of the upper 140 m.

METHODS

Interstitial Water Chemistry

The methods used for the analysis of major and minor constituents of the interstitial waters have been described in the Leg 152 *Initial Reports* (Larsen, Saunders, Clift, et al., 1994), and the data also were published in that volume.

Strontium Isotopes

Sr was separated from pore water samples by a standard ion chromatography technique, using AG50W × 8 (BioRad) cation exchange
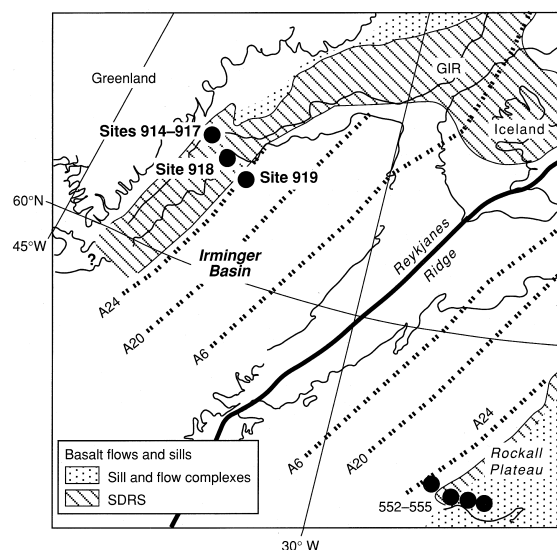

Figure 1. Position map of shelf sites, Leg 152 (Larsen, Saunders, Clift, et al., 1994).

[2]Scripps Institution of Oceanography, University of California, La Jolla, CA 92093-0215, U.S.A. jgieskes@ucsd.edu
[3]Department of Geological Sciences, Princeton University, Princeton, NJ 08544, U.S.A.
[4]Department of Geology and Geophysics, Louisiana State University, Baton Rouge, LA 70803-4101, U.S.A.
[5]Department of Earth Sciences, Boston University, Boston, MA 02215, U.S.A.

resin. The eluted Sr fraction was mixed with 20 μl of 0.025 M H_3PO_4 and evaporated to dryness. The residue was taken up in ~3 μl of 1 M HNO_3 for loading on a prebaked Re filament. Isotopic measurements were made on a 90° sector thermal ionization mass spectrometer, Finnigan MAT 262, using double Re filaments. Data were acquired using simultaneous collection with multi-Faraday cups. The $^{87}Sr/^{86}Sr$ ratios were normalized to $^{86}Sr/^{88}Sr = 0.1194$. One hundred ratios were collected in 10 blocks for each sample and the in-run precision ($2\sigma_m$) is better than ±0.00001 or ~0.0014%. Time series measurements of NBS (National Bureau of Standards) 987 yielded an average value of $^{87}Sr/^{86}Sr = 0.710262 \pm 7$ (n = 12, $2\sigma_m$). The results from replicate analyses of modern seawater are $^{87}Sr/^{86}Sr = 0.709177 \pm 5$ (n = 7, σ_m).

Oxygen Isotopes

Five cm^3 of each sample of interstitial water was sealed in a glass ampoule and transported to the Princeton Stable Isotope Laboratory for oxygen isotope analysis using a modified VG Isoprep18 automated Shaker/Equilibrator. Samples were equilibrated with approximately 100 mmoles of CO_2 at 25°C for 24 hr before analysis on a VG Optima gas source mass spectrometer. The standard deviation of 12 replicate analyses of standard water analyzed at the same time as the interstitial waters is 0.03 per mil.

Lithium Isotopes

Li was separated from other ions by a standard ion chromatographic technique. Li was then converted to Li phosphate and loaded on a pre-baked Re filament. Li isotopic measurement was made on a 90° sector thermal ionization mass spectrometer, Finnigan MAT 262, using double Re filaments. Data were measured directly on ^6Li and ^7Li using peak jumping mode. The ionization filament temperature was controlled at 1300°−1350°C during measurement. The sample size for the measurement was about 100 ng. The blank was about 0.2 ng and was insignificant. Isotopic compositions are expressed as δ^6Li relative to the Li standard L-SVEC ($^6Li/^7Li = 0.08261$). Detailed chemical separation and mass spectrometric procedures are reported in You and Chan (1996). Estimated accuracy is ±1‰.

RESULTS

The oxygen isotope data ($\delta^{18}O[H_2O]$) for Sites 914, 915, and 916 are presented in Table 1. In Table 2 the $\delta^{18}O(H_2O)$, the $^{87}Sr/^{86}Sr$, and the δ^6Li data for Sites 918 and 919 are presented.

DISCUSSION
Shelf Sites

The main reason for the poor recovery in Sites 914, 915, and 916 was the occurrence of glacial debris below the first 10–20 m of the sediment column, resulting from the ice-rafting of coarse to very coarse materials (boulders) to this shallow area of the Greenland shelf (Larsen et al., 1994). The chemistry of the interstitial waters is described in more detail elsewhere (Larsen, Saunders, Clift, et al., 1994). Here we emphasize the observations on dissolved calcium, magnesium, chloride, and $\delta^{18}O(H_2O)$.

Changes with depth in dissolved calcium are relatively small, though generally indicating distinct increases (Fig. 2) The increases in calcium are to some extent balanced by decreases in dissolved magnesium, though no simple relationship between these two constituents is apparent (Fig. 3). Typically, however, similar changes have been interpreted in terms of alteration of volcanic or igneous material in the sediment column or in the underlying basalts (Gieskes and Lawrence, 1981; McDuff, 1981; Lawrence and Gieskes, 1981).

Table 1. Oxygen isotope data for Sites 914, 915, and 916.

Core, section, interval (cm)	$\delta^{18}O$ (H_2O) (‰)
152-914A-	
15R-1, 69–77	−1.41
17R-4, 140–150	−1.57
152-915A-	
1R-1, 145–150	−0.07
18R-1, 140–150	−4.65
19R-2, 140–150	−4.53
21R-2, 46–56	−5.27
152-916A-	
13R-3, 140–150	−7.98

Table 2. Oxygen, strontium, and lithium isotope data for Sites 918 and 919.

| Core, section, interval (cm)	Depth (mbsf)	$^{87}Sr/^{86}Sr$	$\delta^{18}O(H_2O)$ (‰)	δ^6Li (‰)
152-918A-				
2H-4, 140–150	7.8	0.709053		−36.4
4H-4, 145–150	26.8	0.709070		−41.4
7H-1, 0–20	49.3		0.14	
7H-4, 145–150	55.3	0.709074	0.05	−41.4
10H-4, 145–150	83.8	0.709095	−0.03	
12H-1, 0–20	96.8			
13H-4, 145–150	112.3	0.709160		
16H-4, 140–150	139.3	0.709019	−0.48; −0.49	−38.7
17H-1, 0–20	142.8	0.709040	−0.51	
19H-4, 140–150	167.8	0.708954	−0.65; −0.78	−35.4; −33.4
22X-1, 0–20	191.1			
23X-4, 140–150	206	0.708899		−36.9; −35.9
26X-4, 140–150	232	0.708929		−31.5; −28.3
31X-1, 0–20	276	0.709167	−1.17	−28.7
37X-6, 90–100	322	0.709043		−35.6; −33.7
152-918B-				
1H-3, 145–150	4.5			
2H-4, 145–150	12.8		0.25	
3H-5, 145–150	23.8			
152-918C-				
1H-4, 145–150	30			
152-918D-				
13R-1, 0–5	405		−0.97	
22R-2, 140–150	485			
25R-2, 140–150	515	0.708927		
28R-3, 140–150	545		−0.75	
31R-CC	575	0.708189	−0.73	−34.6; −34.4
34R-1, 2–10	602		−0.66; −0.62	
37R-1, 140–150	632	0.708326	−0.55	−30.6
40R-1, 140–150	660	0.708416		−31.2
44R-2, 139–150	700			
47R-1, 50–60	728	0.708467		−27.5; −24.9
51R-2, 140–150	765	0.708550	−0.69	−23.9; −28.2
55R-4, 112–122	803			
62R-1, 121–129	875		−1.43	
68R-1, 91–100	930	0.708382	−1.16	−35.4; −37.5
74R-1, 3–14	985		−0.96	
80R-1, 0–11	1045		−1.23	
83R-1, 136–141	1070			
88R-1, 93–100	1125			
91R-1, 119–129	1150	0.707983	−0.54	−24.1; −25.4
95R-2, 140–150	1183		−0.96	
151-919A–				
1H-2, 145–150	3		0.05	
1H-4, 145–150	6	0.709099	0.03	−39.1
2H-2, 145–150	11	0.709091	0.09	−41.4
2H-4, 145–150	14		0.28; 0.11; 0.195	
3H-2, 145–150	20.5		0.23	
3H-4, 145–150	23.5		0.09; 0.27; 0.18	
4H-2, 145–150	30		0.37	−41.1
4H-4, 145–150	33		0.22; 0.08; 0.15	
5H-2, 145–150	39.5		0.05	
5H-4, 145–150	42.5		0.04	
6H-3, 145–150	50.5	0.709038	0.03; 0.00; 0.015	−41.9
7H-3, 145–150	60	0.709037	−0.12	−36.1
8H-3, 145–150	69.5	0.709008	−0.18	−33.1
9H-3, 145–150	79	0.709007	−0.31; −0.20; −0.255	−33.0
10H-3, 145–150	88.5	0.708950	−0.44; −0.26; −0.35	−31.9
152-919B-				
3H–3, 145–150	94.5	0.708947	−0.29	−36.4; −36.3
4H-3, 145–150	104	0.708950		−30.4
7H-3, 145–150	132.5	0.709014	−0.51	−32.8; −33.6; −32.1
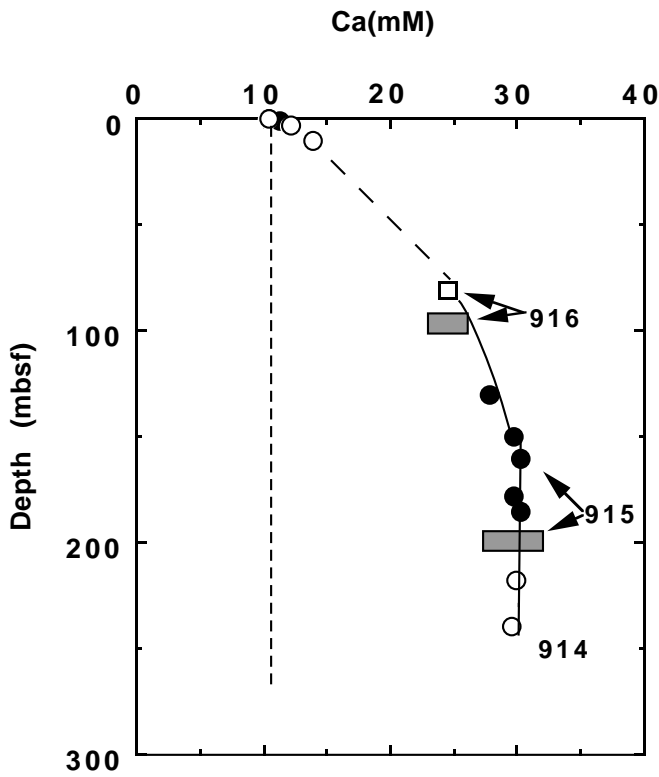
Figure 2. Concentration-depth profiles of dissolved calcium of shelf Sites 914, 915, and 916. Horizontal bars represent location of basement. Dashed line represents seawater calcium.
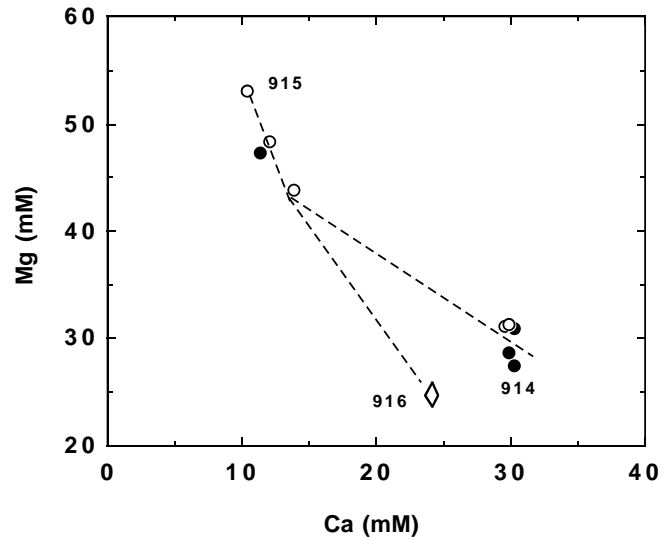

Figure 3. Correlation plot of calcium and magnesium for Sites 914, 915, and 916.
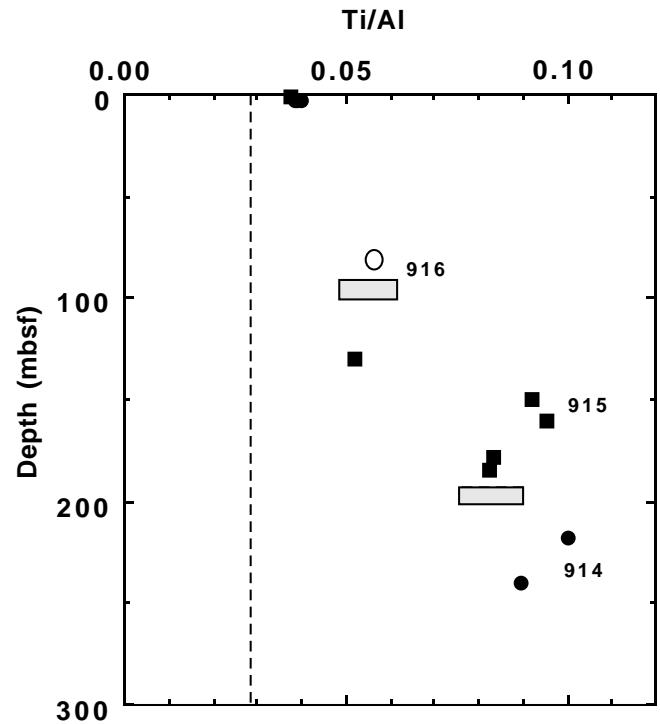

Figure 4. Ti/Al vs. depth plot of bulk analysis of squeezed cakes, Sites 914, 915, and 916. Vertical dashed line is average continental crust value (Wedepohl, 1995).

Murray et al. (this volume) report the major and minor element contents of the bulk sediments of these sites. High ratios of Ti/Al are typical for these sediments (Fig. 4), indicating the presence of volcanic sedimentary sources. Such high Ti/Al ratios also characterize many sediments around Iceland, as has been demonstrated from the chemical analysis of sediments from Deep Sea Drilling Project (DSDP) Leg 38 in the Norwegian-Greenland seas (Gieskes et al., 1987) and Site 907 of Leg 151 (Myhre, Thiede, Firth, et al., 1995). High contributions of basic volcanic ash were implied in the Leg 38 studies, and similar high inputs of volcanic material must be present in the shelf sediments off the coast of Greenland in this study area. It is not known how much the data below the glaciomarine sections are affected by diffusive exchange with the surface sediments, especially because of the lack of information on the potential diffusive permeability of the glaciomarine section. If this communication is sluggish, then it can be concluded that alteration of volcanic material in the deeper sections of the sediments has had relatively little effect on the shallow interstitial water chemistry. This would, of course, render the indicated curvature in Figure 2 rather hypothetical.

Of particular interest are the observations on the depth distributions of dissolved chloride and $\delta^{18}O$ of the pore fluids. The decreases in chloride are quite large, particularly at Site 916, and these decreases are accompanied by large changes in the oxygen isotope ratio (Fig. 5). Two main processes are responsible for these observations: (1) The low chlorides can be understood in terms of a meteoric water input, which would also explain the large decrease in $\delta^{18}O(H_2O)$; (2) Because of the implied alteration of volcanic material in the sediment column, there can also occur a depletion in the $\delta^{18}O(H_2O)$. The latter has been demonstrated by Lawrence and Gieskes (1981) and by Lawrence (1989).

A plot of $\delta^{18}O$ vs. Cl is presented in Figure 6. Unfortunately, we are not in a position to estimate the contribution by volcanic matter

alteration to the oxygen isotope signal, so that the extrapolation to meteoric water values is purely speculative. Epstein and Mayeda (1953) suggest that the melt waters of present-day Greenland have a $\delta^{18}O$ of about −20‰. With this in mind we have drawn the reference line in Figure 6. If, however, the meteoric water is Paleocene in origin and is released from water reservoirs originally formed in the basalt during their subaerial exposure about 55 m.y. ago, we are in no position to estimate the appropriate reference line. As will be demonstrated in the section on the Irminger Basin, Site 918 is also characterized
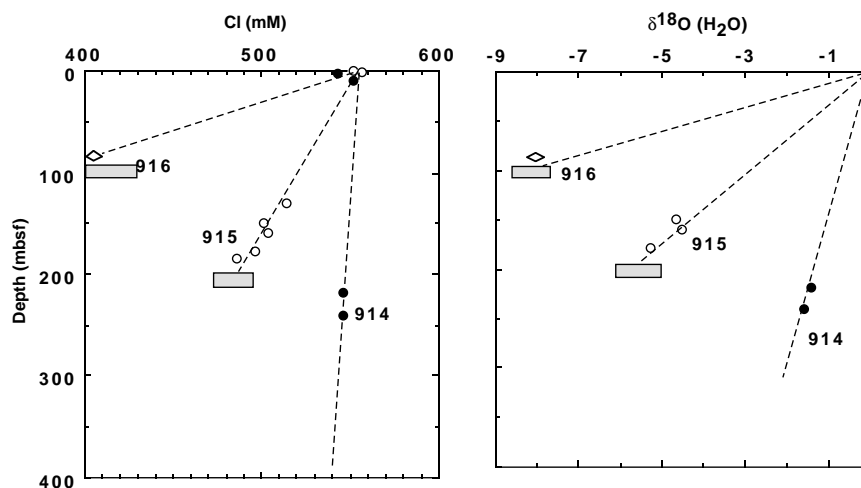
Figure 5. Chloride and $\delta^{18}O(H_2O)$ of pore fluids of Sites 914, 915, and 916. Horizontal bars indicate location of basement.

by low chloride inputs at depth, and during the last re-entry attempt, the hole was noticed to collapse, perhaps as a result of fresh water flow from a buried reservoir in the basalts (Ron Grout, pers. comm., 1994). This would argue for a potential contribution of a freshwater reservoir in the basalts, rather than through an aquifer from Greenland.

Irminger Basin Sites 918 and 919

In these two sites sediment recovery was generally successful enough to allow a reasonably detailed interstitial water study. In addition to a general evaluation of the pore water chemistry, particular attention was paid to a detailed sampling of the upper 150 m of Site 919, with the aim of establishing a possible record of Pleistocene salinity and concurrent oxygen isotope changes of seawater (McDuff, 1985; Schrag and DePaolo, 1993).

It is important to consider the sedimentation rates for these two sites, particularly that of Site 918 (Fig. 7). It is evident that, in the upper section of the sediment column, very high average sedimentation rates (>90 m/m.y.) prevail, but that substantially lower rates characterize the deeper parts of the sediment column. Indeed the sedimentation rate of the section between 100 and 500 meters below seafloor (mbsf) may have been close to 180 m/m.y. (Larsen, Saunders, Clift, et al., 1994). The data on the $^{87}Sr/^{86}Sr$ isotope ratio of biogenic carbonates (Israelson and Spezzaferri, this volume) and paleomagnetic data (Fukuma, Chapter 22, this volume) suggest slightly higher sedimentation rates in the sediments drilled at Site 919, when compared to the upper section of Site 918. Sediments of such high accumulation rates establish a barrier to rapid diffusion, as is evident, for instance, from a calculation of the diffusive path length over the last 5 m.y., that is, $(2Dt)^{1/2} = \sim 245$ m, assuming a diffusion coefficient of 2.10^{-6} cm^2/s. Over this time period roughly 450 m of sediment has accumulated, thus exceeding the diffusive path length by almost a factor of 2. Any signals in the pore fluids caused by relatively recent reactions in the deeper sections will, therefore, penetrate only to a limited extent into the upper sediment column.

The sediments of Sites 918 and 919, like those of the shelf sites, are characterized by the presence of volcanic matter, as is evident from the variable, but high, Ti/Al ratios of the bulk sediments. These depth distributions are presented in Figure 8 (see also Murray et al., this volume). In addition Site 918 has also been investigated in detail for its bulk chemical composition (Saito, this volume). Again the evidence for the presence of high Ti/Al volcanic material is clear from these data. A plot of the ratio of Ti/Al vs. that of Fe/Al (Murray et al., this volume) suggests a similar origin of the volcanic component in the shelf and basin sediments (Fig. 9). The presence of a fairly large amount of volcanic matter might lead to substantial alteration of this
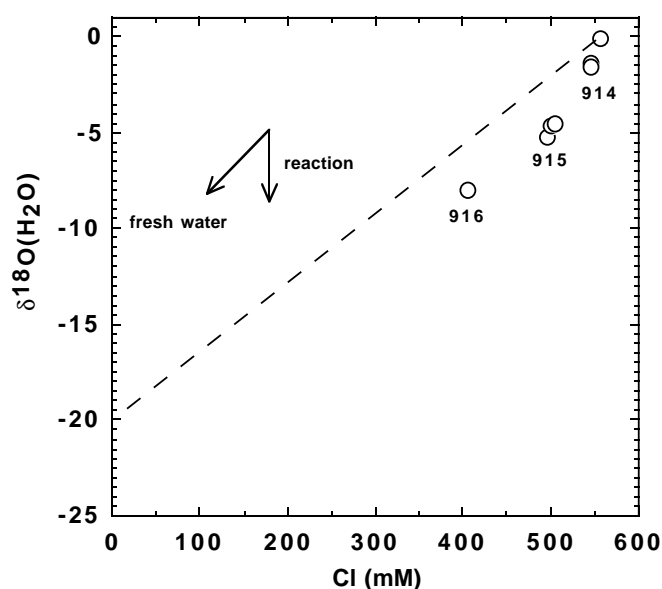

Figure 6. Correlation plot of $\delta^{18}O(H_2O)$ vs. chloride of pore fluids of Sites 914, 915, and 916. Dashed line indicates proposed extrapolation to local meteoric water.

material in the sediment column, as was demonstrated for the sediments of the Norwegian-Greenland Seas by Gieskes et al. (1987).

Major Cationic Constituents

Alkaline Earths

The concentration-depth profiles of the alkaline earth metals are presented in Figure 10. In essence, the profiles in Site 919 provide a similar distribution as in the upper 150 m of Site 918. Thus similar processes have affected these constituents in the upper part of the rapidly deposited sediment section. Decreases in calcium can be understood in terms of calcium carbonate precipitation caused by the large increases in alkalinity (mostly bicarbonate) associated with the decomposition of organic carbon. Rapid decreases in magnesium may, in part, be due to some carbonate precipitation, but more likely are the result of the incorporation of magnesium in clay minerals during the alteration of volcanic matter in these sediments. Typically these sediments of the upper part of Sites 918 and 919 are characterized by relatively low values of the strontium isotope ratio, when compared
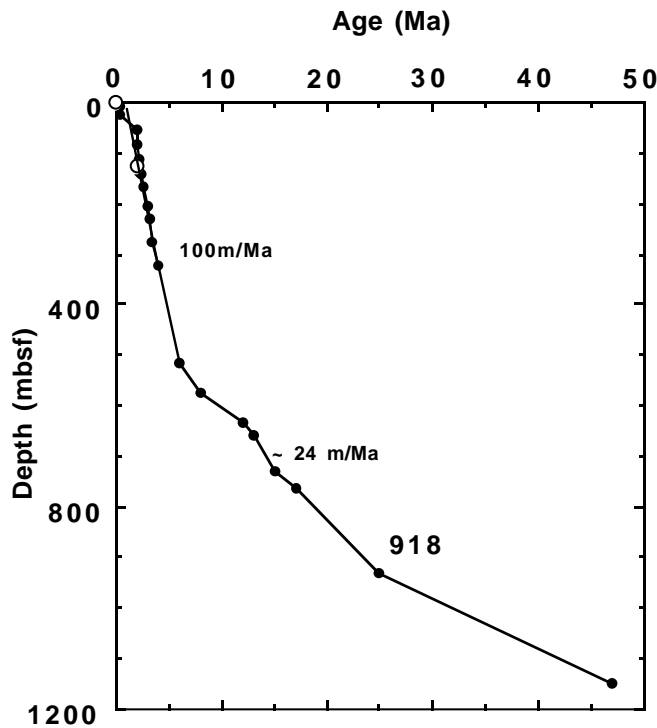
Figure 7. Sedimentation rate diagram for Site 918 (Larsen, Saunders, Clift, et al., 1994).
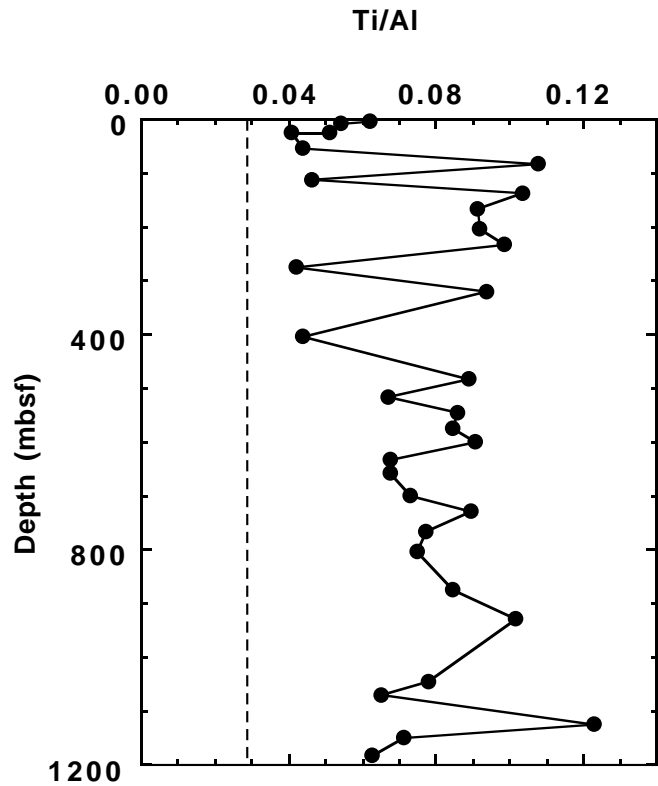

Figure 8. Ti/Al vs. depth plot of bulk analysis of squeezed cakes, Site 918. Vertical dashed line is average continental crust value (Wedepohl, 1995).
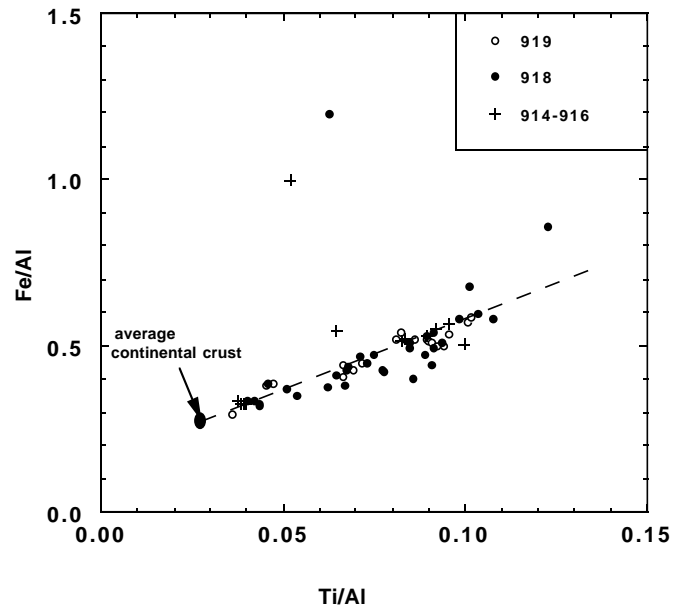

Figure 9. Correlation between Ti/Al and Fe/Al for bulk sediment analysis of squeezed cakes (Murray et al., this volume), Sites 914, 915, 916, 918, and 919. Oval represents average continental crust (Wedepohl, 1995).

with the contemporaneous seawater values (see below), testifying to the isotopic exchange between sedimentary pore fluids and altering volcanic matter. Notwithstanding this, dissolved strontium also decreases with depth in these upper sections, possibly as a result of incorporation in precipitating authigenic calcium carbonate. However, typically the ratio of the decrease in strontium to that in dissolved calcium is ~4 mmol/mol, much higher than the ratio expected in authigenic marine carbonates (0.3–0.6 mmol/mol; Delaney, 1989). Perhaps a portion of the strontium is also taken up in clay minerals during sediment alteration processes. The observation that dissolved strontium is removed, but yet is influenced by nonradiogenic strontium stemming from volcanic material, suggests that the dissolved components are not necessarily a quantitative measure of sediment-interstitial water interactions.

Below 200 mbsf reversals occur in the profiles of calcium and magnesium, leading to extrema in their concentrations at about 550 mbsf. Dissolved strontium presents a more complicated profile, although there is a broad secondary minimum in the zone of the extrema at 550 mbsf. The extrema suggest that reactions in this horizon occur that lead to the release of calcium and the uptake of magnesium, most likely as a result of volcanic matter alteration. Below, the observations on concentration changes in potassium, sodium, chloride, as well as in the $^{87}Sr/^{86}Sr$ isotope ratio support this interpretation. A plot of calcium vs. magnesium (Fig. 11) also suggests that diffusive mixing above and below the extrema leads to linear trends, thus emphasizing the very narrow reaction zone in these sediments.

Alkali Metals

The concentration depth patterns of the dissolved alkali metals (Fig. 12) indicate very similar profiles in the upper 150 m of the sediment column at both sites. Typically, the data in the upper 150 m of Site 919 are again reflected in those of the upper part of Site 918. Of importance to note is the very rapid decrease in dissolved lithium, the almost linear decreases in potassium, and the almost constancy in dis-
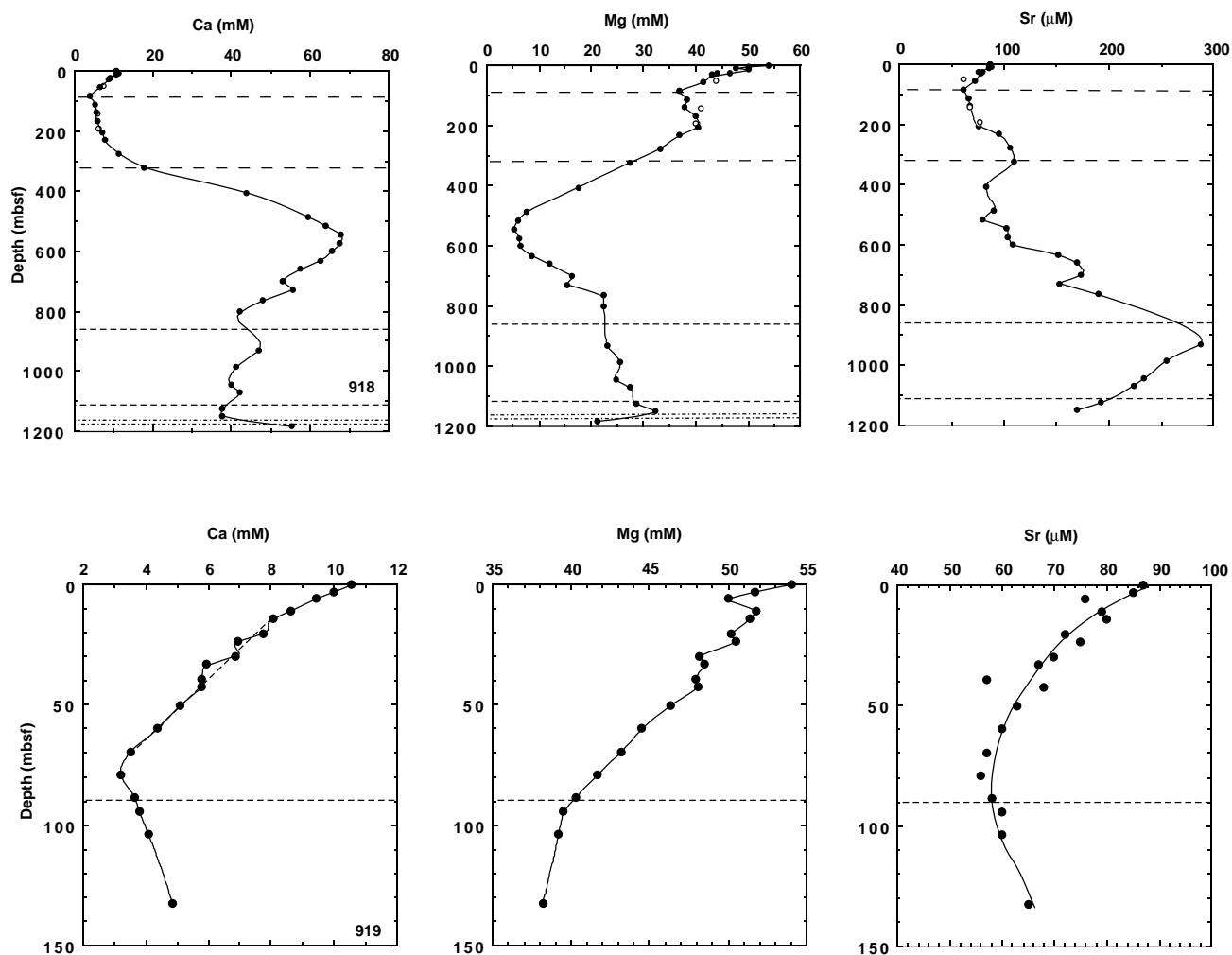
Figure 10. Depth distribution of alkaline earths in pore waters of Sites 918 and 919. Open circles = in situ values. For Site 918: section between 90 and 310 mbsf is the methane zone; 860–1120 mbsf is sandy turbidites; sill at ~1170 mbsf. For Site 919: start of methane zone is at 90 mbsf.
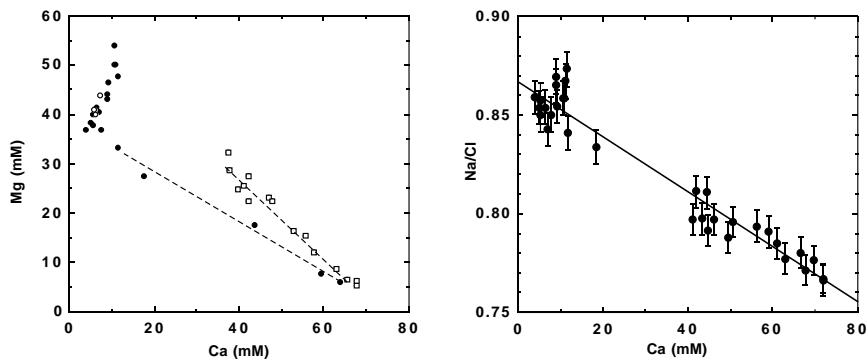
Figure 11. Correlation plots of Ca vs. Mg and Ca vs. Na/Cl at Site 918. Solid circles = above 550 mbsf; open circles = in situ values; open squares = below 550 mbsf.

solved sodium. Decreases in lithium have also been observed in the interstitial waters of the upper part of the sediment column of Site 808 in the Nankai Trough. Other sites that show the shallow decrease in lithium are sites in the Vanuatu Basin (Martin, 1994). The decrease in lithium cannot simply be explained in terms of coprecipitation with carbonate. Typically carbonates have Li/Ca ratios of less than 20.10^{-6} mol/mol, whereas the decreases observed in this study would "correspond" to dissolved calcium decreases in a ratio of about 2.10^{-3} mol/mol. In addition, dissolved calcium decreases do not correlate

well with those in dissolved lithium. An alternate explanation may be sought in the uptake of Li by carbonate during recrystallization, as has been demonstrated in almost pure carbonate sediments in the Pacific Ocean (Chen-Feng You, pers. comm., 1996). However, this process is not a likely sink for the Li because of the low carbonate contents (<<10%) of these drill sites in the upper 150 mbsf (Larsen, Saunders, Clift, et al., 1994). A more likely cause is the alteration of volcanic material leading to the removal of pore water lithium into the alteration phases. The low $^{87}Sr/^{86}Sr$ ratios support this interpreta-
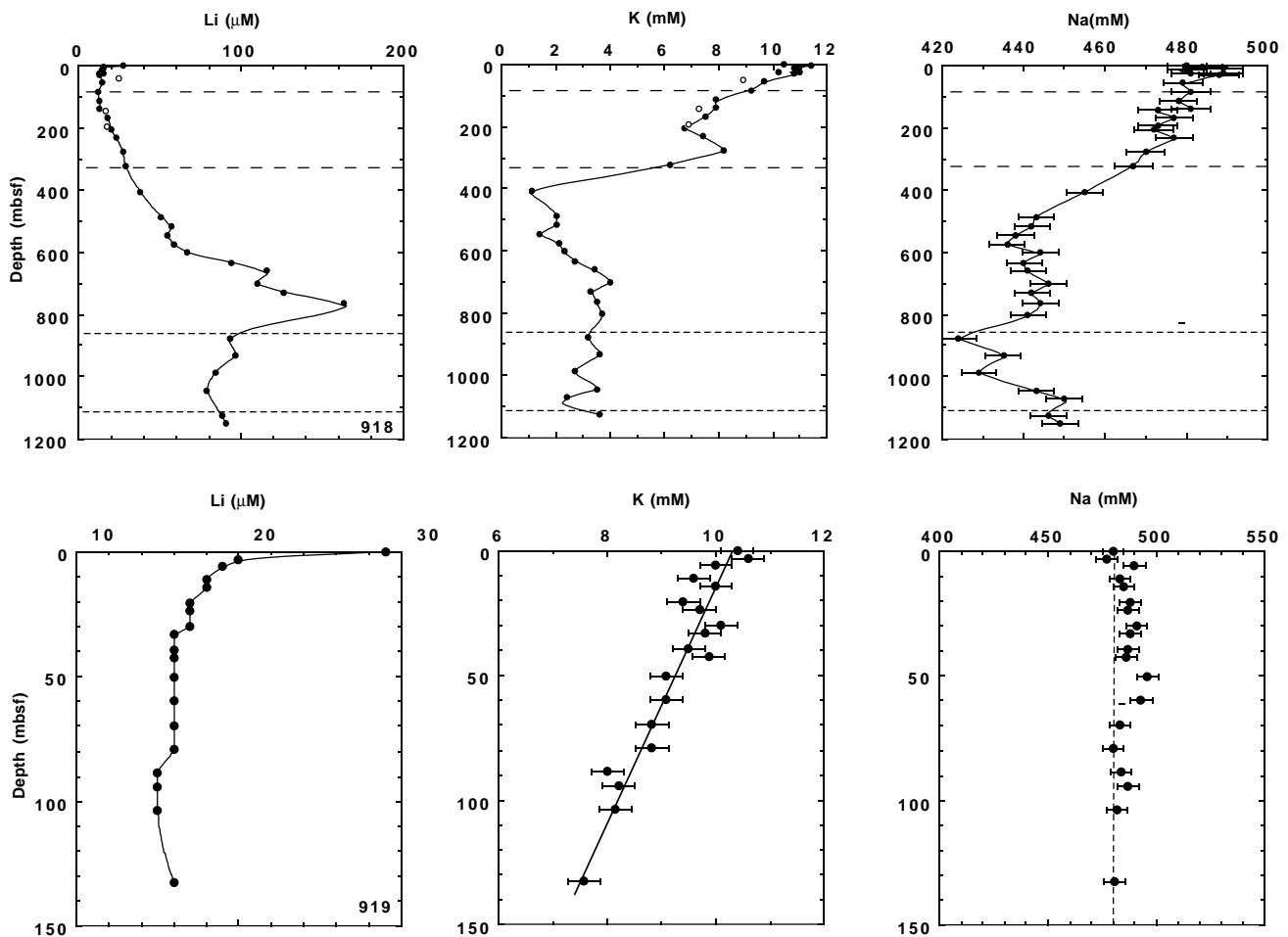
Figure 12. Depth distribution of alkali metals in pore waters of Sites 918 and 919. Open circles = in situ values. For Site 918: section between 90 and 310 mbsf is the methane zone; 860−1120 mbsf is sandy turbidites. For Site 919: start of methane zone is at 90 mbsf.

tion. At low temperatures, basalts, which have undergone low temperature alteration, have been shown to act as a sink for Li (e.g., Mengel and Hoefs, 1990).

The concentration depth profiles in the deeper sections, however, show interesting trends. Dissolved lithium gradually increases with depth below ~150 mbsf at Site 918 to reach a maximum at a depth of ~750 mbsf. The lower values in the deeper units are probably related to the advective inputs of lower lithium containing fluids in the underlying sandstones (see discussion on chloride contents, below). Dissolved potassium shows a minimum at ~200 mbsf, an intermediate maximum at 300 mbsf, and a minimum at ~550 mbsf (i.e., in the zone characterized by the extrema in calcium and magnesium), and is the result of uptake during the alteration of volcanic matter. Similarly dissolved sodium shows a minimum in the reaction zone at ~550 mbsf. To investigate the nature of the dissolved sodium gradient, however, it is appropriate to investigate the depth profile of Na/Cl, because of the fairly large variations in dissolved chloride observed, especially at Site 918.

Chloride and Na/Cl

The chloride and Na/Cl depth profiles are presented in Figure 13. In the upper part of the sediment column of both Sites 918 and 919 a distinct dissolved chloride maximum occurs, at ~25 mbsf at Site 918 (~565 mM) and at ~50 mbsf (~572 mM) at Site 919. Especially at Site 919 the maximum is well defined. Below, we will elaborate on this

phenomenon in greater detail, but it is related to the recent higher glacial salinity signal (McDuff, 1985; Schrag and DePaolo, 1993).

At greater depths, however, chloride shows a broad maximum around the 550 mbsf level. This can be attributed to the same phenomenon that has been invoked for the observations on the calcium and magnesium extrema. Uptake of water into clay minerals during volcanic matter alteration must be invoked to explain these increases in chloride. An increase of 2.5% in dissolved chloride is well above the analytical uncertainty of better than 0.3%.

A gradual decrease in chloride occurs below 600 mbsf, but below 820 mbsf (i.e., in the sandy layers) large fluctuations in dissolved chloride occur. These fluctuations can be understood in terms of possible advection of fluids along the sandy horizons, with a potential cause being the input of fresh waters from basement toward the slope of the basin, or advection of low chloride fluids from the shelf. As Site 918 is located at a much greater water depth than the shelf sites, the former explanation is more likely.

The sodium data have been normalized to chloride to remove the effects of the chloride variations, which are considered to be mostly due to uptake or release of fresh water (at least in the deeper sections). The Na/Cl ratio shows a very clear minimum at 550 mbsf, confirming the occurrence of the sodium concentration minimum in these horizons. The sodium concentration profile (as well as that of Na/Cl) shows a distinct decrease below ~130 mbsf. This decrease starts earlier than the decrease in dissolved chloride. It is not certain whether these differences are due to analytical uncertainties or whether indeed
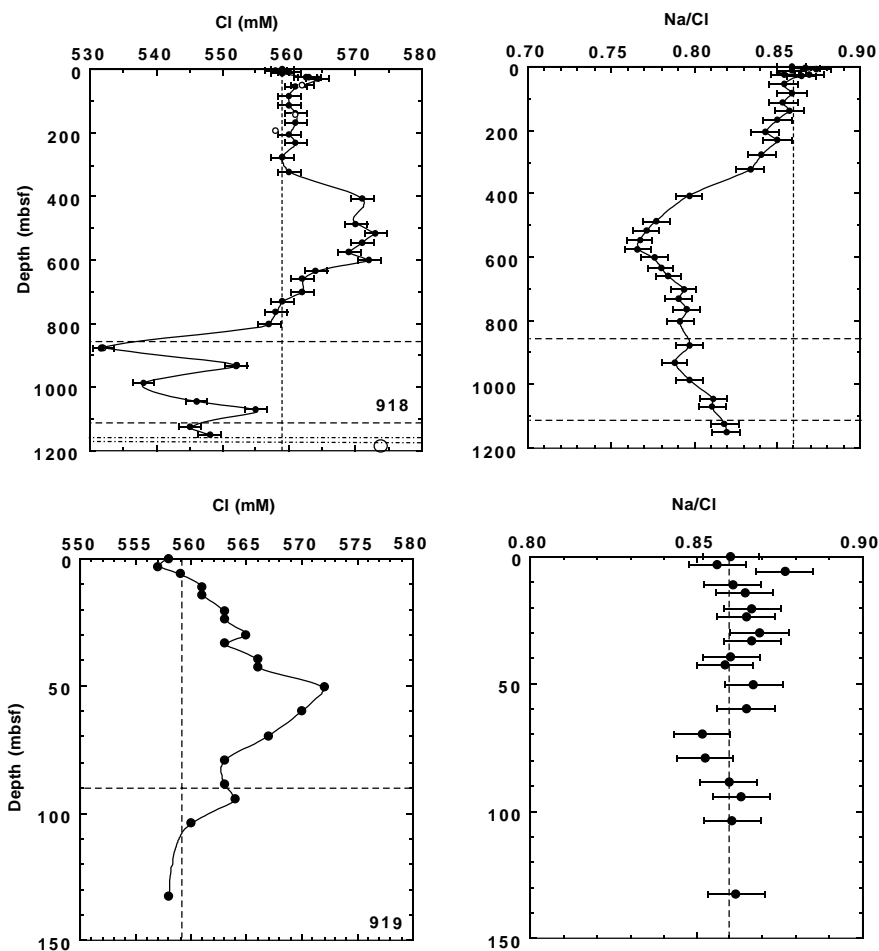
299

Figure 13. Depth distributions of chloride and Na/Cl at Sites 918 and 919 (annotations same as Fig. 10). Large circle is data point below sills.

diffusive transport to or from the reaction zone at 550 mbsf has led to these differences.

A correlation between the concentrations of dissolved calcium and the Na/Cl ratio (Fig. 11) again strongly suggests that reactions responsible for the concentration extrema in calcium and magnesium are also the cause of the changes in sodium.

Strontium and Strontium Isotopes

The study of the stable isotope ratio $^{87}Sr/^{86}Sr$ of dissolved strontium is of importance in any evaluation of the processes that lead to the observed changes in interstitial water chemistry. After the first measurements of interstitial water strontium isotopes by Lawrence et al. (1979), the database has been expanded to include many DSDP drill sites (Elderfield and Gieskes, 1982). In volcanic matter-rich sediments there is strong evidence that alteration of volcanic material in the sediment column has led to a substantial lowering of the ratio below contemporaneous values (Gieskes et al., 1986, 1987; von Breymann et al., 1991; Martin, 1994). The signal, particularly in carbonate-rich sediments, can become complicated as a result of the release of strontium during carbonate recrystallization (Gieskes et al., 1986; Martin, 1994). At Site 833 of the Vanuatu Basin, for example, Martin (1994) found very high concentrations of dissolved strontium (up to 2500 µM) in a carbonate section of the hole, and as a result of this process very high strontium isotope ratios occur, notwithstanding large potential contributions of volcanic matter alteration.

The $^{87}Sr/^{86}Sr$ isotope ratios of dissolved strontium of Sites 918 and 919 are presented in Figure 14. It is evident that various zones occur in the sediment column that have undergone isotopic exchange with volcanic matter of low $^{87}Sr/^{86}Sr$ composition: (1) the upper 100 m of

the sediments in both sites; (2) a zone centered around ~200 mbsf at Site 918; and (3) a more strongly affected zone centered at 550 mbsf at Site 918. The upper two reaction zones do not show correlative changes in dissolved calcium and magnesium (Fig. 11), but the zone centered around 550 mbsf has already been recognized as a reaction zone characterized by large changes in calcium, magnesium, potassium, sodium, and chloride.

At Site 919 there appears to be a rough correlation between dissolved lithium and the strontium isotope ratio of dissolved strontium (Fig. 15). This observation could confirm the interpretation offered above that alteration of igneous material in the upper sediments is the cause of the observed lithium decrease.

Of special interest is the observation that studies of the strontium isotope stratigraphy of well-preserved specimens of foraminifers of planktonic and benthonic origin (Israelson and Spezzaferri, this volume), show a remarkably good agreement with paleontologically established ages throughout Site 918. In the sediments of Site 919 the $^{87}Sr/^{86}Sr$ stratigraphy appears most reliable. This suggests that the calcium carbonate skeletons in these sediments are not necessarily in isotopic equilibrium with the pore fluids. Indeed, any recrystallization would lead to a trend toward contemporaneous seawater values (Martin, 1994). At depths below 800 mbsf, however, pore water ratios are elevated above the contemporaneous seawater values. These are also the sediments in which moderate acid leaches show elevated values of the strontium isotope ratio (Israelson and Spezzaferri, this volume). Thus, a contribution of more radiogenic strontium could be associated with alteration of this more radiogenic material. A maximum in dissolved Sr does occur at ~925 mbsf. The fluids advected through these sediment layers have been interpreted in terms of low chloride fluids stemming from reservoirs in the basalts. However,
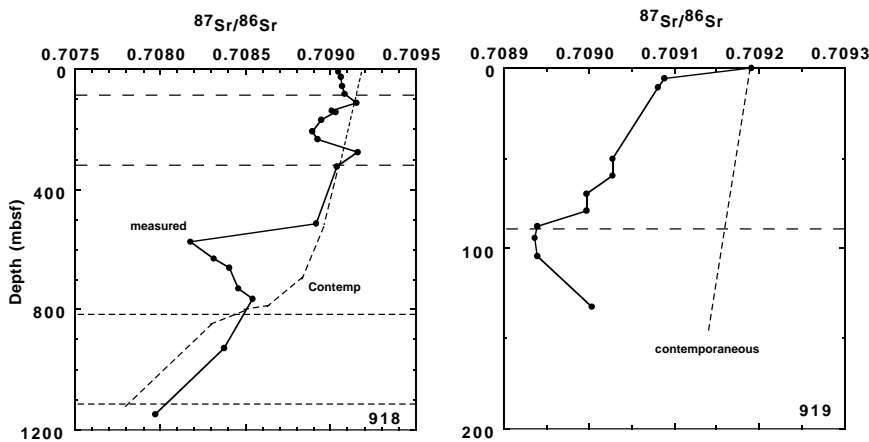
Figure 14. $^{87}Sr/^{86}Sr$ of dissolved strontium at Sites 918 and 919. For contemporaneous values, see Israelson and Spezzaferri (this volume).
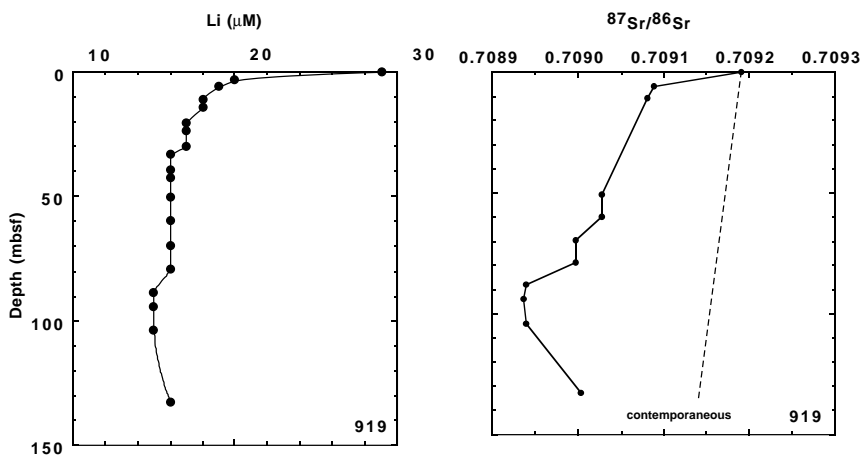

Figure 15. Depth distribution of lithium and $^{87}Sr/^{86}Sr$ in pore waters of Site 919.

these reservoirs should have lesser radiogenic signatures. If diffusive processes are of importance below 925 mbsf, the higher $^{87}Sr/^{86}Sr$ ratios could also be due to diffusion from the maximum at 925 mbsf. In carbonate sites, heavier strontium isotopes in the pore waters at greater depths have previously been explained in terms of such diffusive exchange processes (Gieskes et al., 1986). A similar interpretation cannot be offered readily here, because a major problem is that as a result of the advection of fluids below ~820 mbsf, the gradient in strontium may not simply be caused by diffusive processes alone.

Oxygen Isotopes in the Pore Fluids

A detailed analysis of the distribution of $\delta^{18}O(H_2O)$ has been conducted, both for the pore fluids collected in the shelf sites (see discussion above) and at Sites 918 and 919. The data for these latter sites are presented in Figure 16. Details in the upper part of Site 918 are not adequate to establish the exact location of the maximum in the upper part of the hole, but the data at Site 919 show very clear evidence for a maximum at ~25 mbsf. Below these maxima, however, a rapid decrease is observed in the $\delta^{18}O(H_2O)$, with a minimum at Site 918 at ~250 mbsf. Again the similarities in the profiles of the upper parts of Sites 918 and 919 are striking. The occurrence of extrema in the depth distributions of calcium, magnesium, and sodium at Site 918 had led us to the expectation of an extremum in the distribution of $\delta^{18}O$ at the depth of ~550 mbsf, especially because of the low $^{87}Sr/^{86}Sr$ ratios in this interval. Such a decrease is not evident from the distribution in Figure 16. Processes responsible for the minimum at ~250 mbsf dominate the $\delta^{18}O$ profile in the upper 700 m of the sediment column. Below, we will elaborate on this phenomenon in greater detail.

Pleistocene Oxygen Isotope Signal

The upper sections of Sites 918 and 919 are of interest because of the possibility of the detection of a Pleistocene glacial signal in the salinity and $\delta^{18}O(H_2O)$ as discussed in detail by McDuff (1985) and Schrag and DePaolo (1993). The data for chloride and $\delta^{18}O$ are plotted in Figure 17. Especially at Site 919 there occurs a distinct maximum in dissolved chloride (2.3% enrichment), but at Site 918 a much less pronounced signal occurs. Data for the $\delta^{18}O$, on the other hand, show similar characteristics. Of special note, however, is that at Site 919 the maxima in chloride and $\delta^{18}O$ do not occur at the same depths. For chloride it occurs at ~50 mbsf, but for $\delta^{18}O$ at ~25 mbsf. The problem, of course, is that for the two signals different boundary conditions occur. Whereas the chloride concentration below the maximum returns to the seawater value, for $\delta^{18}O$ there is a pronounced minimum at ~250 mbsf (Fig. 16). As a result, the maximum in $\delta^{18}O$ would shift upward. In addition, small differences in diffusion coefficients may also play a minor role. Thus, even though a glacial signal can be discerned in the pore water profiles of chloride and $\delta^{18}O$, the situation becomes more complicated because of the more complex nature of the distribution of $\delta^{18}O$. Similar observations can be inferred from the data of McDuff (1985), who established a chloride maximum at ~40 mbsf and a $\delta^{18}O$ maximum at ~25 mbsf, with boundary conditions not unlike those of the present study.

Significance of the Deeper $\delta^{18}O(H_2O)$ Profile

The data for the entire Site 918, both for dissolved chloride and for $\delta^{18}O(H_2O)$, are presented in Figure 18. Figure 19 shows the plots of $\delta^{18}O(H_2O)$ and $^{87}Sr/^{86}Sr$ of dissolved strontium. Whereas in the up-

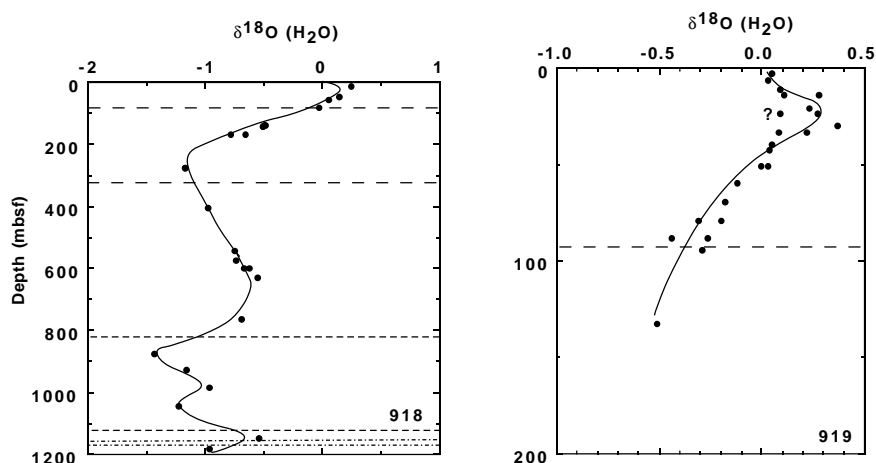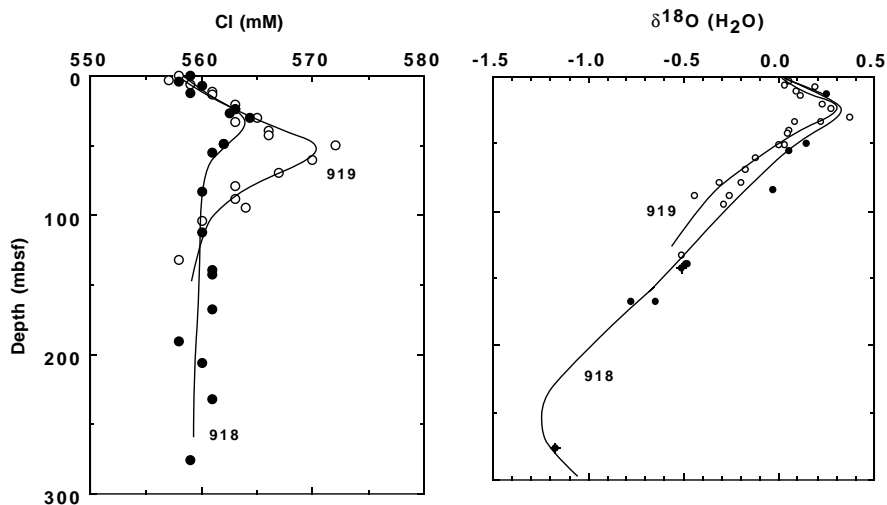Figure 16. Depth distributions of δ¹⁸O(H₂O) at Sites 918 and 919 (annotations same as Fig. 10).

Figure 17. Depth distributions of chloride and δ¹⁸O(H₂O) in upper 300 mbsf of Sites 918 and 919. Solid circles = Site 918; open circles = Site 919.

per 300 mbsf the chloride profile shows only a slight maximum, the increase in chloride below 300 mbsf indicates a broad maximum centered around 550 mbsf. Deviations in the isotope ratio in the upper 300 m of the sediment column suggest the presence of alteration of volcanic material in these sediments, though no particularly large anomalies occur in the inorganic constituents in these depths, but for a minimum in magnesium at ~100 mbsf and in potassium at ~200 mbsf. The minimum in δ¹⁸O(H₂O), however, is relatively large and centered around 250 mbsf or perhaps a little shallower. The latter is suggested by the minimum in ⁸⁷Sr/⁸⁶Sr at ~210 mbsf. Thus the low δ¹⁸O(H₂O) occurs in the middle of the zone of methane generation. At Site 808 of the Nankai Trough a low value of δ¹⁸O(H₂O) = –4.5‰ was observed at 151 mbsf in the upper part of a thick sequence of trench turbidites (Kastner et al., 1993). This low value was also not accompanied by large changes in cationic compositions (except for an increase in dissolved sodium), but ⁸⁷Sr/⁸⁶Sr values of dissolved strontium were below contemporaneous values. The low value of the δ¹⁸O(H₂O) was explained in terms of hydration reactions involving clay mineral formation resulting from volcanic matter alteration. Recrystallization of carbonate, which is relatively sparse in this upper section of the site (<5%), cannot explain this decrease in δ¹⁸O(H₂O) (Lawrence, 1989). Indeed, the most likely candidate for the observed minimum at ~250 mbsf is the hydration of neo-formed clay minerals. Thus, notwithstanding the absence of any large signals in most cations, or in dissolved chloride, the uptake of ¹⁸O at ~250 mbsf must be more important quantitatively than in the horizon at ~550 mbsf. This argument is based on the usefulness of δ¹⁸O as a quantitative indicator, the reservoir of oxygen in the pore fluids being close to that of the

solid phases (Lawrence et al., 1975; Lawrence, 1989). Clearly, quantitative estimates of the degree of volcanic matter alteration should not be based on the changes in cationic concentrations or even in dissolved chloride, which show the largest changes in the 550 mbsf horizon. Interestingly this is also the horizon where glacial dropstones (543.5 mbsf) disappear from the sediments, and where mineralogical composition data also indicate a change in sediment composition (Vallier et al., this volume). Associated with that change are clear geochemical changes in the sediments (Saito, this volume). Certainly volcanic matter alteration in this depth horizon is of importance, as is also borne out by the minimum in ⁸⁷Sr/⁸⁶Sr (Fig. 19), but the minimum at ~250 mbsf dominates the δ¹⁸O distribution.

Below 800 mbsf (i.e., in the zones characterized by the occurrence of large depletions in chloride; Fig. 17) also variations in δ¹⁸O(H₂O) occur. We argued previously that these chloride depletions could best be understood in terms of advective fluid input, characterized by low chloride and also by low δ¹⁸O(H₂O). A meteoric water origin, as proposed for the shelf sites, is the most likely source for these anomalies, perhaps originating in the underlying basement toward the Greenland Margin or as a result of advection along an aquifer from the land. The latter, however, is highly unlikely in this situation. As before, the former explanation is favored here.

Lithium Isotopes in the Pore Fluids

Data for the depth distribution of lithium isotopes at Sites 918 and 919 are presented in Figure 20. Solid circles and open circles represent duplicate measurements.
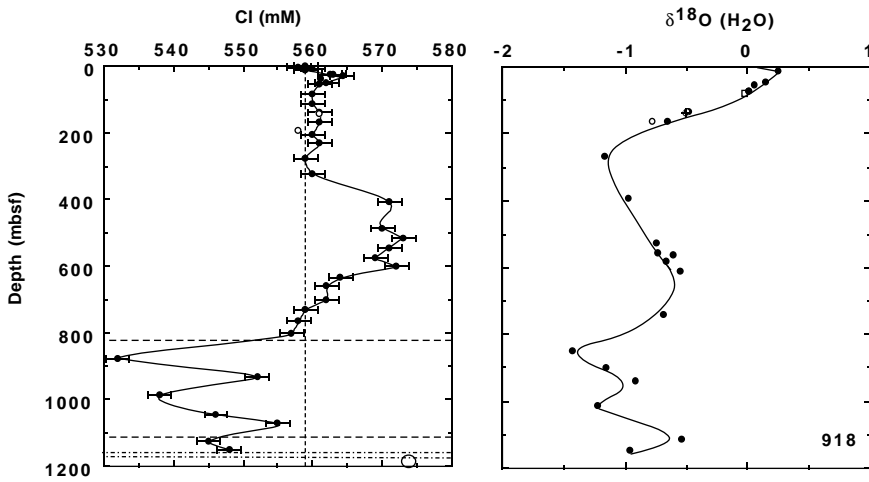
Figure 18. Depth distributions of chloride and $\delta^{18}O(H_2O)$ at Site 918 (annotations same as Fig. 10). Large circle is data point below sills.

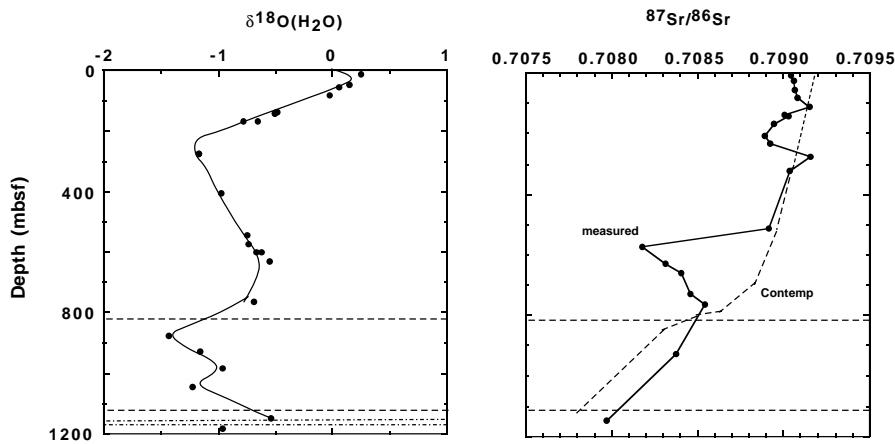Figure 19. Depth distributions of $\delta^{18}O(H_2O)$ and $^{87}Sr/^{86}Sr$ at Site 918 (annotations same as Fig. 10).
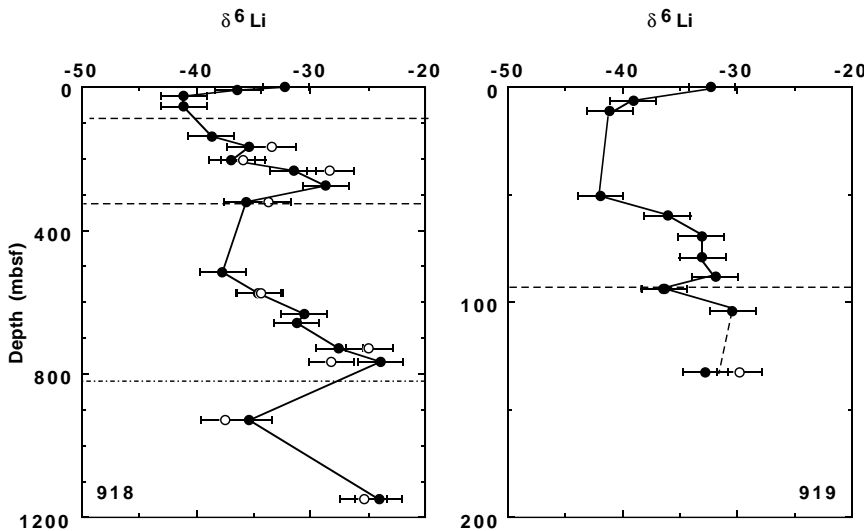

Figure 20. Depth distributions at Sites 918 and 919 of pore water lithium isotopes. Solid circles and open circles represent duplicate measurements.

Based on Ca and Mg concentrations and Sr isotopic data, we propose two potential processes that are responsible for the observed changes in the Li isotope distribution: alteration of volcanic materials and the precipitation of calcite. Provided that the precipitation of calcite accounts for the decrease of Ca and that the Li/Ca molar ratio in the calcite is 20×10^{-6}, the Li concentration of pore water should decrease at the most by 0.2 μM (compare with Fig. 12). The precipita-

tion of calcite, therefore, can be considered minor in terms of affecting the Li concentration and isotopic composition. The Li concentration decreases to about half of the seawater value within the upper 100 m. The decrease can be explained by the uptake of Li during the alteration of volcanic material. The alteration products preferentially incorporate the light Li isotope (Chan et al., 1992). This is consistent with the observed shift to heavier isotopic composition of the pore

waters compared to that of the seawater (−32.3‰; Chan and Edmond, 1988).

Around the depth of 250 mbsf (Site 918), $^{87}Sr/^{86}Sr$ and $\delta^{18}O$ minima indicate the alteration of volcanic materials. However, the δ^6Li returns to the seawater value. The δ^6Li maximum corresponds to a NH_4^+ maximum in the zone of zero sulfate concentrations (methane zone). This correlation is also observed at Site 919. Because the NH_4^+ extrema are associated with the microbial decomposition of organic material, the light Li isotopic composition might in part be derived from organic materials. In addition, the significant amount of NH_4^+ produced can undergo exchange with cations in clay minerals (Gieskes, 1983). Because Li and Sr concentrations are in the mM range, the exchange of NH_4^+ with cations in clay minerals may have a significant effect on Li and Sr isotopic compositions of the pore water. A small Sr concentration maximum and more radiogenic Sr isotopic composition are observed at ~300 mbsf. Similarly, Li may be expelled from the exchangeable positions in clay minerals, causing the observed shift to lighter isotopic compositions in the pore waters.

A δ^6Li minimum is present at ~500 mbsf, coinciding with the strong $^{87}Sr/^{86}Sr$ minimum caused by volcanic alteration. From 500 to 800 mbsf, the Li concentration increases with depth. Experimental studies (You, 1994; Chan et al., 1994) have shown that Li can be released from the marine sediments at temperatures as low as 50°−60°C. The release of Li from the sediments at elevated temperatures could account for the Li enrichment at depth. The alteration of volcanic materials, which takes up Li from the interstitial water, appears to be minor compared to the release from the sediments. δ^6Li in the pore water increases steadily from 500 to 800 mbsf and correlates with 1/Li ($r2 = 0.869$), suggesting two-component mixing, with one component having a δ^6Li of −21‰, which is attributable to sediment-derived Li. The δ^6Li of pelagic clays ranges from −10‰ to −14‰ (Chan et al., 1994). This correlation suggests different degrees of Li release at different depths accompanied by isotopic fractionation.

Into the sandy section of the hole (800 to ~1100 mbsf), Li concentration decreases and δ^6Li shifts to −36.6‰. These largely reflect reduced input from the sediments at this horizon. The advecting fresh water with low Li levels would not significantly affect the Li isotopic composition in this layer.

At the base of Hole 916, the Li concentration of the pore water is 9.0 mM with a δ^6Li of −26.6‰. The concentration would be 12.4 mM after correction for dilution by fresh water based on the Cl concentration. There is therefore a decrease from the seawater concentration, which can be attributed to the alteration of volcanic material. On the other hand, the uptake of Li by alteration minerals should result in a heavier isotopic composition than seawater. The relatively light Li isotopic composition observed at this site is not readily explained.

SUMMARY AND CONCLUSIONS

Several important aspects of the studies on the interstitial waters obtained in the drill sites along the margin transect of Greenland drilled during Leg 152 can be summarized as follows:

1. For a more complete understanding of the processes responsible for the chemical changes in the composition of interstitial waters, it is necessary not only to study the inorganic chemical composition of the dissolved salts, but it is equally necessary to study stable isotopes, in particular those of dissolved strontium ($^{87}Sr/^{86}Sr$) and of the oxygen isotopic composition of the pore waters $\delta^{18}O(H_2O)$. This has been demonstrated before by various authors (Lawrence et al., 1975, 1979; Gieskes et al., 1982, 1987). The study of the $\delta^{18}O(H_2O)$ clearly indicates that a major reaction zone is located at a depth of approximately 250 mbsf. The observed minimum in $\delta^{18}O$ is not likely the result of carbonate diagenesis or organic matter alteration, thus suggesting that the process leading to this minimum is associated with volcanic matter alteration. Particularly at Site 918 the distribution of $\delta^{18}O$ indicates that volcanic matter alteration is not always reflected in a quantitative manner by changes in the major ion chemical composition.

2. The data obtained in the study of Site 918 suggest the presence of three reaction zones involving the alteration of volcanic matter in the sediments. The first is located in the near surface sediments (low $^{87}Sr/^{86}Sr$), the second is located around the depth horizon between 200 and 250 mbsf (lower $^{87}Sr/^{86}Sr$ and minimum in $\delta^{18}O$), and the third zone is between 500 and 600 mbsf (extrema in major components and lowest $^{87}Sr/^{86}Sr$). The data on the Ti/Al ratio of the sediments (see also Murray et al. and Saito, both this volume) suggest the presence of volcanic matter throughout the site, but of some interest are the distinct maxima in K_2O, Rb, and Th in the sediments from the reaction zones (Saito, this volume), particularly the sediments just below the 500 mbsf barrier, below which sedimentation rates show a rapid decrease. We do not, at this time, understand the potential relationship between these observations, but there is no doubt that these anomalies do correspond to the reaction zones observed in the pore fluids.

3. In the upper 100 m of the interstitial water column maxima in $\delta^{18}O(H_2O)$ and chloride attest to the presence of a Holocene seawater signal (higher $\delta^{18}O(H_2O)$ and chloride concentration). The offset between the depths at which these extrema occur is a function of the different boundary conditions for these components.

4. Observations in the shelf Sites 914−916 and in the deeper parts of Site 918 strongly suggest an input of meteoric waters into the sediments, evidenced particularly by the lowering of the chloride contents and the occurrence of low $\delta^{18}O(H_2O)$. It is not certain whether the origin of the fresh water is due to input from an aquifer bringing in recent meltwaters from Greenland or whether the fluids are from freshwater reservoirs trapped within basaltic basement while this was subaerially exposed prior to basin subsidence.

5. Studies of lithium isotopes in the pore fluids of Sites 918 and 919 indicate a great deal of complexity, indicating the importance of both volcanic matter alteration (uptake of Li) and of release from the sediments at greater depths. This is the first detailed investigation of the lithium isotope geochemistry in pore fluids of deep drill cores.

ACKNOWLEDGMENTS

REFERENCES

Chan, L.H., and Edmond, J.M., 1988. Variation in the lithium isotope composition in the marine environment. *Geochim. Cosmochim. Acta,* 52:1711−1717.

Chan, L.H., Edmond, J.M., Tompson, G., and Gillis, K., 1992. Lithium isotopic composition of submarine basalts: implications for the lithium cycle in the oceans. *Earth Planet. Sci. Lett.,* 108:151−160.

Chan, L.H., Gieskes, J.M., You, C.F., and Edmond, J.M., 1994. Lithium isotope geochemistry of sediments and hydrothermal fluids of the Guaymas Basin, Gulf of California, *Geochim. Cosmochim. Acta,* 58:4443−4454.

Chan, L.H., Zhang, L., and Hein, J.R., 1994. Lithium isotope characteristics of marine sediments. *Eos,* 75:314.

Delaney, M.L., 1989. Temporal changes in interstitial water chemistry and calcite recrystallization in marine sediments. *Earth Planet. Sci. Lett.,* 95:23−37.

Elderfield, H., and Gieskes, J.M., 1982. Sr isotopes in interstitial waters of marine sediments from Deep Sea Drilling Project cores. *Nature,* 300:493−497.

Epstein, S., and Mayeda, T., 1953. Variation of ^{18}O content of waters from natural sources. *Geochim. Cosmochim. Acta,* 4:213−224.

Gieskes, J.M., 1983. The chemistry of interstitial waters of deep-sea sediments: interpretation of deep-sea drilling data. *In* Riley, J.P., and Chester, R. (Eds.), *Chemical Oceanography* (Vol. 8): London (Academic), 222−269.

Gieskes, J.M., Elderfield, H., Lawrence, J.R., Johnson, J., Meyers, B., and Campbell, A., 1982. Geochemistry of interstitial waters and sediments, Leg 64, Gulf of California. *In* Curray, J.R., Moore, D.G., et al., *Init. Repts. DSDP,* 64 (Pt. 2): Washington (U.S. Govt. Printing Office), 675−694.

Gieskes, J.M., Elderfield, H., and Palmer, M.R., 1986. Strontium and its isotopic composition in interstitial waters of marine carbonate sediments. *Earth Planet. Sci. Lett.,* 77:229−235.

Gieskes, J.M., and Lawrence, J.R., 1981. Alteration of volcanic matter in deep-sea sediments: evidence from the chemical composition of interstitial waters from deep sea drilling cores. *Geochim. Cosmochim. Acta,* 45:1687−1703.

Gieskes, J.M., Lawrence, J.R., Perry, E.A., Grady, S.J., and Elderfield, H., 1987. Chemistry of interstitial waters and sediments in the Norwegian-Greenland Sea, Deep Sea Drilling Project Leg 38. *Chem. Geol.,* 63:143−155.

Kastner, M., Elderfield, H., Jenkins, W.J., Gieskes, J.M., and Gamo, T., 1993. Geochemical and isotopic evidence for fluid flow in the western Nankai subduction zone, Japan. *In* Hill, I.A., Taira, A., Firth, J.V., et al., *Proc. ODP, Sci. Results,* 131: College Station, TX (Ocean Drilling Program), 397−413.

Larsen, H.C., Saunders, A.D., Clift, P.D., et al., 1994. *Proc. ODP, Init. Repts.,* 152: College Station, TX (Ocean Drilling Program).

Larsen, H.C., Saunders, A.D., Clift, P.D., Beget, J., Wei, W., Spezzaferri, S., and the ODP Leg 152 Scientific Party, 1994. Seven million years of glaciation in Greenland. *Science,* 264:952−955.

Lawrence, J.R., 1989. The stable isotope geochemistry of deep-sea pore water. *In* Fritz, P., and Fontes, J.C. (Eds.), *Handbook of Environmental Isotope Geochemistry* (Vol. 3) (2nd ed): Amsterdam (Elsevier), 317−356.

Lawrence, J.R., Drever, J.I., Anderson, T.F., and Brueckner, H.K., 1979. Importance of alteration of volcanic material in the sediments of Deep Sea Drilling Site 323: chemistry, $^{18}O/^{16}O$ and $^{87}Sr/^{86}Sr$. *Geochim. Cosmochim. Acta,* 43:573−588.

Lawrence, J.R., and Gieskes, J.M., 1981. Constraints on water transport and alteration in the oceanic crust from the isotopic composition of pore water. *J. Geophys. Res.,* 86:7924−7934.

Lawrence, J.R., Gieskes, J.M., and Broecker, W.S., 1975. Oxygen isotope and cation composition of DSDP pore waters and the alteration of Layer II basalts. *Earth Planet. Sci. Lett.,* 27:1−10.

Martin, J.B., 1994. Diagenesis and hydrology at the New Hebrides Forearc and intra-arc Aoba Basin. *In* Greene, H.G., Collot, J.-Y., Stokking, L.B., et al., *Proc. ODP, Sci. Results,* 134: College Station, TX (Ocean Drilling Program), 109−130.

McDuff, R.E., 1981. Major cation gradients in DSDP interstitial waters: the role of diffusive exchange between seawater and upper oceanic crust. *Geochim. Cosmochim. Acta,* 45:1705−1713.

——, 1985. The chemistry of interstitial waters, Deep Sea Drilling Project Leg 86. *In* Heath, G.R., Burckle, L.H., et al., *Init. Repts. DSDP,* 86: Washington (U.S. Govt. Printing Office), 675−687.

Mengel, K., and Hoefs, J., 1990. Li-δ^{18}O-SiO$_2$ systematics in volcanic rocks and mafic lower crustal granulite xenoliths. *Earth Planet. Sci. Lett.,* 101:42−53.

Myhre, A.M., Thiede, J., Firth, J.V., et al., 1995. *Proc. ODP, Init. Repts.,* 151: College Station, TX (Ocean Drilling Program).

Schrag, D.P., and DePaolo, D.J., 1993. Determination of δ^{18}O of seawater in the deep ocean during the last glacial maximum. *Paleoceanography,* 8:1−6.

von Breymann, M.T., Swart, P.K., Brass, G.W., and Berner, U., 1991. Pore-water chemistry of the Sulu and Celebes Seas: extensive diagenetic reactions at Sites 767 and 768. *In* Silver, E.A., Rangin, C., von Breymann, M.T., et al., *Proc. ODP, Sci. Results,* 124: College Station, TX (Ocean Drilling Program), 203−215.

Wedepohl, K.H., 1995. The composition of the continental crust. *Geochim. Cosmochim. Acta,* 59:1217−1232.

You, C.F., 1994. Lithium, beryllium, and boron isotope geochemistry: implications for fluid processes in convergent margins [Ph.D. thesis]. Univ. of California, San Diego.

You, C.F., and Chan, L.H., 1996. Precise determination of lithium isotopic composition in low concentration natural samples. *Geochim. Cosmochim. Acta*, 60:909−915.